Magnetic Resonance Imaging, Vol. 17, No. 8, pp. 1121–1133, 1999

Printed in the USA.
0730-725X/99 $–see front matter

ELSEVIER

PII S0730-725X(99)00048-X

● *Original Contribution*

VISUALIZING AND CHARACTERIZING WHITE MATTER FIBER STRUCTURE AND ARCHITECTURE IN THE HUMAN PYRAMIDAL TRACT USING DIFFUSION TENSOR MRI

ANETTE VIRTA, ALAN BARNETT, AND CARLO PIERPAOLI

Neuroimaging Branch, NINDS, National Institutes of Health, Bethesda, MD, USA

We used diffusion tensor imaging to assess diffusion anisotropy in the pyramidal tract in ten young, and ten elderly subjects (five males and five females in each group). The purpose of this study was to define normative values for anisotropy at different anatomic levels of the brainstem as well as to assess differences due to age, gender, and laterality. In all subjects, anisotropy was highest in the cerebral peduncle, lowest in the caudal pons, and intermediate in the medulla. In the pons and medulla the regional variability was high, with significant differences in anisotropy even between contiguous slices. Multifactorial ANOVA (performed using the average value of anisotropy within each region of interest) revealed that elderly subjects had significantly lower values than young subjects in the cerebral peduncle, with no differences in the pons and medulla. No significant differences in anisotropy due to gender and side were found. The differences in anisotropy at different levels of the brainstem reflect differences in the local architecture of white matter fibers. Anisotropy is high in the cerebral peduncle because fibers have a highly ordered arrangement, while in the pons and medulla, anisotropy is lower because the local fiber architecture is less coherent due to the presence of other fibers and nuclei. The biologic meaning of the intergroup differences in anisotropy is discussed in light of the structure and architecture of the tissue under investigation. We also consider potential sources of artifacts, such as noise and motion, partial volume contamination, anatomic mismatching, and the use of inappropriate statistical tests. We conclude that the age-related decrease in anisotropy in the cerebral peduncle is not artifactual but rather reflects subtle structural changes of the aging white matter. Our study however shows that caution must be exercised in interpreting diffusion anisotropy data. **© 1999 Elsevier Science Inc.**

Keywords: **Diffusion MRI; White matter; Anisotropy; Aging; Human.**

INTRODUCTION

Magnetic resonance imaging (MRI) has been increasingly used to study tissue water diffusion in vivo. By acquiring diffusion-weighted images (DWIs) with diffusion gradients oriented in at least six non-collinear directions, it is possible to estimate the diffusion tensor (D) in each voxel.[1] Diffusion tensor data can in turn be used to compute quantities that characterize specific features of the diffusion process, such as the principal diffusivities (eigenvalues of **D**), the trace of the diffusion tensor (Trace(**D**)), indices of diffusion anisotropy, and the principal directions of diffusion (eigenvectors of **D**) (See ref.[2] for a review). These diffusion parameters can provide clinically useful information that is not available from conventional, relaxometry-based MRI. Significant changes of Trace(**D**), which is proportional to the orientationally averaged diffusion coefficient, has been observed in brain ischemia and stroke,[3,4] as well as in normal brain development.[5–7] Anisotropy measures have been shown to provide information about the integrity and structural arrangement of white matter fibers[8,9] that may be useful in investigating several white matter diseases. Using diffusion anisotropy as a diagnostic tool to detect subtle changes in white matter structure, however, is not straightforward and data analysis in particular is complicated by several factors. First, unlike signal intensity in T_1- and T_2- weighted images, diffusion anisotropy varies widely among different white matter regions, re-

RECEIVED 1/25/99; ACCEPTED 4/19/99

Address correspondence to Dr. Carlo Pierpaoli, NICHD, National Institutes of Health, Bldg. 13 Room 3N17, 13 South Drive, Bethesda, Maryland, 20892-5766. E-mail: carlo@helix.nih.gov

flecting differences in fiber-tract architecture.[8] This inherent regional variability makes identification of abnormalities more difficult. Second, thermal noise in the MR images[10] and motion artifacts can severely affect anisotropy measurements. Finally, the clinical use of diffusion anisotropy would necessitate creating normative databases that are presently unavailable.

In this study, we used diffusion tensor MRI in normal volunteers to investigate the descending pathways located in the ventral portion of the brainstem. We use the term "pyramidal tract" to refer to these structures with a broad meaning to include all corticospinal and corticopontine fibers in addition to the fibers originating from the cells of Betz.[11,12]

The main goal of this study was to characterize diffusion anisotropy in the pyramidal tract at different levels of the brainstem, and to assess differences related to age, gender, and laterality. Since postmortem studies in the aged brain indicate moderate neuronal cell loss, replacement gliosis, and loss of myelin,[13] we were particularly interested in determining whether subtle age-associated changes produced detectable anisotropy changes in white matter that appears normal in the conventional MRI. Additionally, we discuss our data in light of the effects that thermal noise and motion artifacts in the DWIs may exert on the quantitative assessment of diffusion anisotropy.

MATERIALS AND METHODS

Subjects

Ten young (aged 24–36 years, mean 29.5) and ten elderly (aged 64–76 years, mean 69.2) healthy volunteers participated in the study. Each age group was composed of five males and five females. All subjects were right-handed with the exception of one young male and one elderly female. Inclusion criteria were: a) normal neurologic examination, and: b) absence of abnormalities in the conventional MRI. However, since focal hyperintensities are extremely common in the T_2-weighted images of healthy elderly subjects,[14,15] small white matter hyperintensities were accepted in this age group provided that they were not located in either the pyramidal tract or the internal capsule.

MRI

All imaging studies were performed with a 1.5 T GE Signa Horizon EchoSpeed spectrometer, equipped with a whole-body gradient coil able to produce gradient pulses up to 22 mT/m and a birdcage quadrature radio-frequency coil (GE Medical Systems, Milwaukee, WI). Head motion was reduced by placing padding on both sides of the subject's head. Diffusion images were acquired with an interleaved spin-echo echo-planar imaging sequence with a navigator echo to correct motion artifacts.[16,17] A description of the algorithms used for image reconstruction is presented elsewhere.[18,19] The following acquisition parameters were used: 30–33 contiguous axial slices; 3.5-mm slice thickness; 220-mm field-of-view; 128 × 128 in-plane resolution (8 interleaves, 16 echoes per interleaf); echo-time of 78 ms; and repetition time of greater than 5 s with cardiac gating (3–4 acquisitions per heart beat starting with a 200 ms delay after the rise of the sphygmic wave as measured with a peripheral pulse oxymeter). We also acquired conventional fast spin echo T_1-, T_2-, and proton density-weighted images matching the slices of the diffusion study, having however a higher in-plane resolution (256 × 256). Six logical gradient directions were sampled,[8] with four images acquired for each direction at maximum gradient strength (21 mT/m), yielding a b-value (i.e., trace of the b-matrix[20]) of 1,006 s/mm^2. Four images with no diffusion gradients were also acquired for a total of 28 images per slice. The total imaging time was approximately 30–40 min depending on the subject's heart rate. Following image reconstruction, we numerically computed the b-matrix for each image[20] and calculated the diffusion tensor (**D**) in each voxel according to Basser et al.[1] From **D** we computed maps of the three principal diffusivities (eigenvalues of **D**) λ_1, λ_2, and λ_3, Trace(**D**), the principal directions of diffusion (eigenvectors of **D**), the "relative" anisotropy index,[21] and the "lattice" anisotropy index.[10] The lattice anisotropy index, LI, is a rotationally invariant measure of diffusion anisotropy that is relatively immune from bias induced by noise in the diffusion-weighted images. It is computed using:

$$\mathrm{LI_N} = \frac{\sqrt{3}}{\sqrt{8}} \frac{\sqrt{D_{\mathrm{ref}} : D_{\mathrm{N}}}}{\sqrt{\mathrm{D_{ref}} : \mathrm{D_N}}} + \frac{3}{4} \frac{D_{\mathrm{ref}} : D_{\mathrm{N}}}{\sqrt{\mathrm{D_{ref}} : \mathrm{D_{ref}}} \sqrt{\mathrm{D_N} : \mathrm{D_N}}} \quad (1)$$

where $\mathrm{D_{ref}}$: $\mathrm{D_N}$ denotes the tensor dot product between the diffusion tensor of the given voxel $\mathrm{D_{ref}}$, and that of the neighboring voxel $\mathrm{D_N}$. *D* (italic) indicates the anisotropic part of the diffusion tensor or "deviatoric" tensor.[21] The formula of the lattice index is reported here because it contained typographical errors in the original publication.[10] A more detailed description of the quantities appearing in the formula, and the properties of the lattice anisotropy index are reported in reference.[10]

Region-of-Interest Analysis

Regions-of-interest (ROIs) were manually drawn on the left and right pyramidal tract on all slices in the brainstem from a level slightly above the red nucleus to a level just above the pyramidal decussation. In the medulla, the left and right pyramidal tract could not be

clearly separated and, therefore, only a single ROI including both structures was drawn. The pyramidal tract was identified on the anisotropy maps. Color maps of fiber direction[22] were also used to identify and exclude from the ROI voxels which contained anisotropic fibers that did not have an orientation consistent with the known orientation of the pyramidal tract, such as the transverse pontine fibers (See Fig. 1). In the brainstem, the pyramidal tract runs in the proximity of cerebrospinal fluid (CSF) containing spaces. To define the boundaries between CSF and tissue, we used objective criteria that do not rely on visual inspection. Since Trace (**D**) is markedly higher in CSF (Trace(**D**) = 9600 $\mu m^2/s$) than in the brain tissue (Trace(**D**) = 1950–2200 $\mu m^2/s$), tissue segmentation procedures based on Trace (**D**) values can be effectively used to differentiate CSF from brain parenchyma.[8] We empirically found that, at the level of the cerebral peduncle and the pons, none of the voxels having Trace(**D**) above 3000 $\mu m^2/s$ was located in the center of the pyramidal tract in any of the subjects. Therefore, we drew the ROIs without attempting to exclude CSF, but then we excluded all voxels having Trace(**D**) above 3000 $\mu m^2/s$ from the analysis. At the level of the medulla, the pyramidal tract is so thin that using this threshold often excluded all voxels in the ROI. Therefore, in the medulla we accepted a higher level of CSF contamination by setting the Trace(**D**) threshold to 3500 $\mu m^2/s$.

Signal-to-noise Ratio and Motion Artifact Index. In each slice, we identified three regions: 1) a region containing either the entire brain or the ROI under investigation (named "object"); 2) a region positioned in the background of the image in the phase encode direction adjacent to the object (named "bp"); and 3) a region positioned in the background of the image in the frequency encode direction (named "bf"). Defining P as the average of the sum of the squares of the signal intensity in all voxels contained in the region, the average signal-to-noise ratio (SNR) for the object region is given by:

$$SNR = \sqrt{P_{object}/P_{bf}} \quad (2)$$

We define the motion artifact index (MA) as

$$MA = (P_{bp} - P_{bf}) * 100/(P_{object}). \quad (3)$$

In the absence of motion artifacts, bp and bf should have similar signal, represented essentially by thermal noise*; therefore, $P_{bp} - P_{bf}$ should be close to zero. Subject motion causes additional ghosts in the phase encode direction in multishot diffusion weighted images. These artifacts can be reduced but not completely eliminated using the parameters measured with navigator echoes. In particular, navigator echoes cannot suppress ghosts due to non-rigid body motion. The result of uncorrected motion is an increase in P_{bp} with no change in P_{bf}, and hence an increase in MA. MA as defined in equation 3 is $P_{bp} - P_{bf}$ normalized with respect to P_{object}, and expressed as a percentage. MA is not a measure of the subject motion, it is instead an index of how corrupted diffusion weighted images are because of uncorrected motion.

Statistical Analysis

Multifactorial ANOVA was used to assess the effect of age, gender, and side (left and right) on diffusion anisotropy, Trace(**D**), and the eigenvalues of **D**. The effect of side was assessed first by including all subjects in the analysis, and then by excluding the two left-handed subjects. The analysis was performed in three anatomic regions of the brainstem (cerebral peduncle, pons, and medulla). For each anatomic region, data from three contiguous slices were included, making every effort to ensure optimal anatomic matching between homologous regions from different subjects (Fig. 1). In the medulla, the effect of side was not tested because left and right ROIs could not be differentiated reliably. For each diffusion parameter, ANOVA was performed first by using the values of the individual voxels included in the anatomic region, and then by using the mean value of each ROI.

The effect of thermal noise and subject motion on anisotropy values was assessed by testing whether a significant correlation existed between lattice anisotropy index and SNR, and between lattice anisotropy index and MA. For this analysis, we used average values of anisotropy, SNR, and MA in the three contiguous slices where the cerebral peduncle ROIs were defined. The "object" region included the whole brain with the exclusion of voxels containing CSF (Trace(**D**) above 3000 $\mu m^2/s$). We also tested for significant differences in SNR and MA among different age and gender groups by performing multifactorial ANOVA on this dataset.

* EPI images are susceptible to artifacts due to differences between even and odd echoes in each echo train. These artifacts consist of ghost images displaced from the main image in the phase encode direction. These ghosts are unrelated to subject's motion and are present even in images acquired with no diffusion weighting. We use parameters obtained from a reference scan, which consists of an EPI acquisition without phase encode blips, to reduce this artifact. In images of a phantom obtained with the same sequence that was used for our diffusion study we found that MA was the order of 0.13%, indicating that the contribution of these ghosts is negligible.

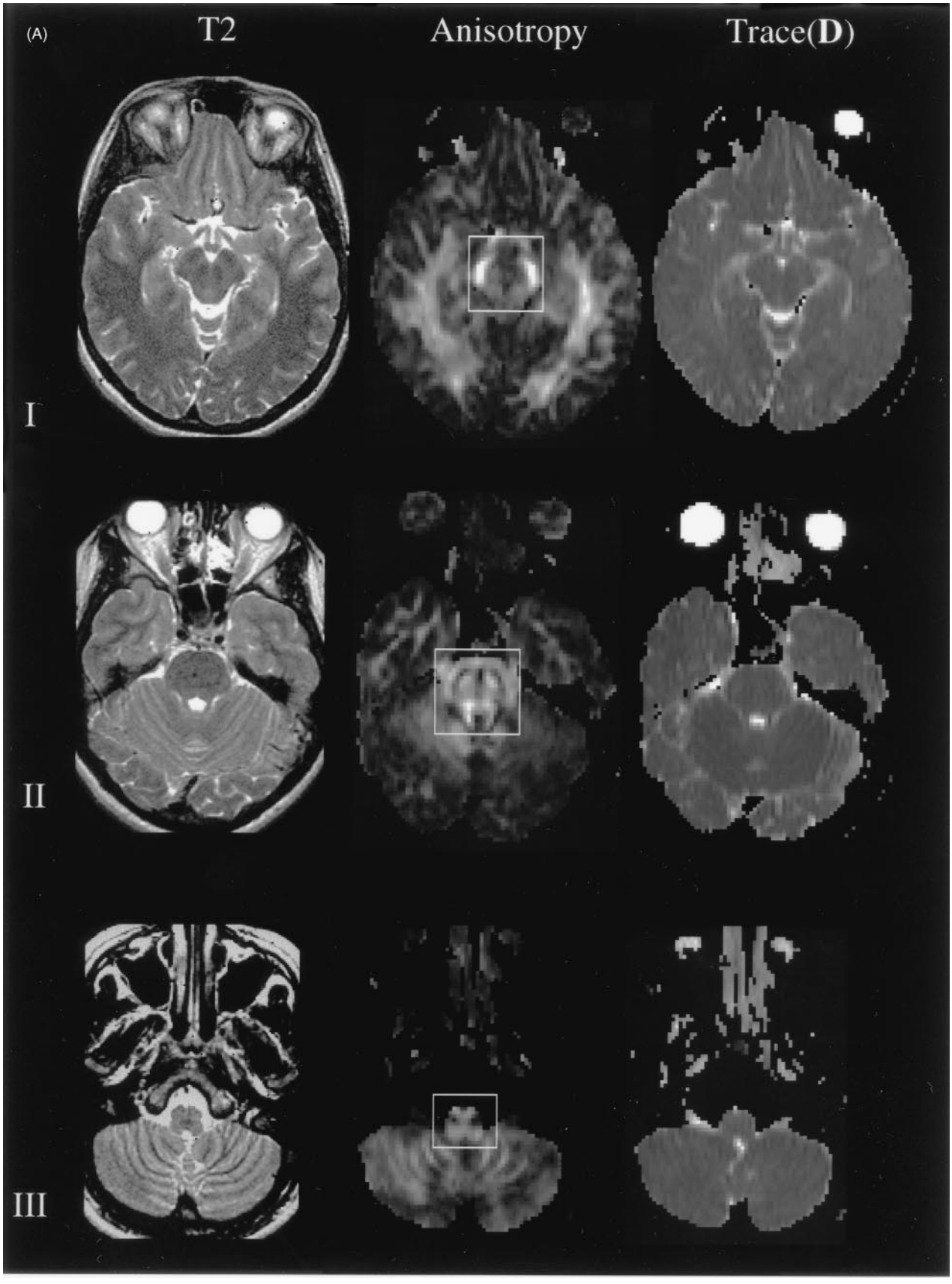
(A)
T2
Anisotropy
Trace(D)
I
II
III

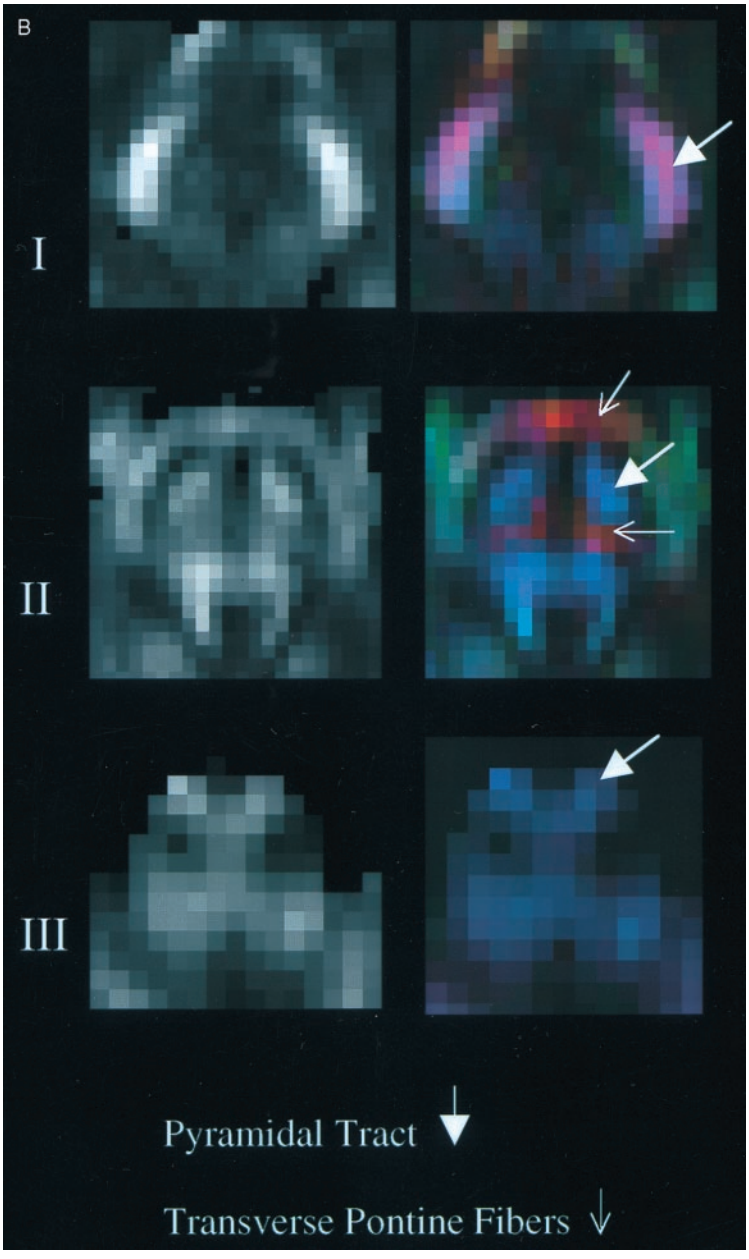

Fig. 1. (A) T_2-weighted images, lattice anisotropy index maps, and Trace(**D**) maps of the cerebral peduncle (I), pons (II), and medulla (III). For each anatomic area, the middle slice of the three slices included in the statistical analysis is shown. The rectangle encloses the region that is presented magnified in (B). In the anisotropy maps, bright voxels indicate high diffusion anisotropy and correspond to white matter fibers whereas dark voxels indicate low anisotropy and correspond to CSF and gray matter. In the Trace(**D**) maps, bright voxels indicate high Trace(**D**) and correspond to CSF, while the dark voxels indicate low Trace(**D**) and corresponds to gray and white matter. (B) Magnified anisotropy and directionally encoded color maps of the cerebral peduncle (I), pons (II), and medulla (III). The color maps show the fiber orientation as indicated by the direction of the eigenvector associated with the largest principal diffusivity (ϵ_1) in each voxel.[22] In this representation, the components of ϵ_1 are associated with the three primary colors: red, green, and blue. Red color corresponds to left-right, green to anterior-posterior, and blue to rostral-caudal fiber orientation. Fibers with oblique orientation are depicted with colors resulting from the combination of the three primary colors. See Reference 22 for additional details.

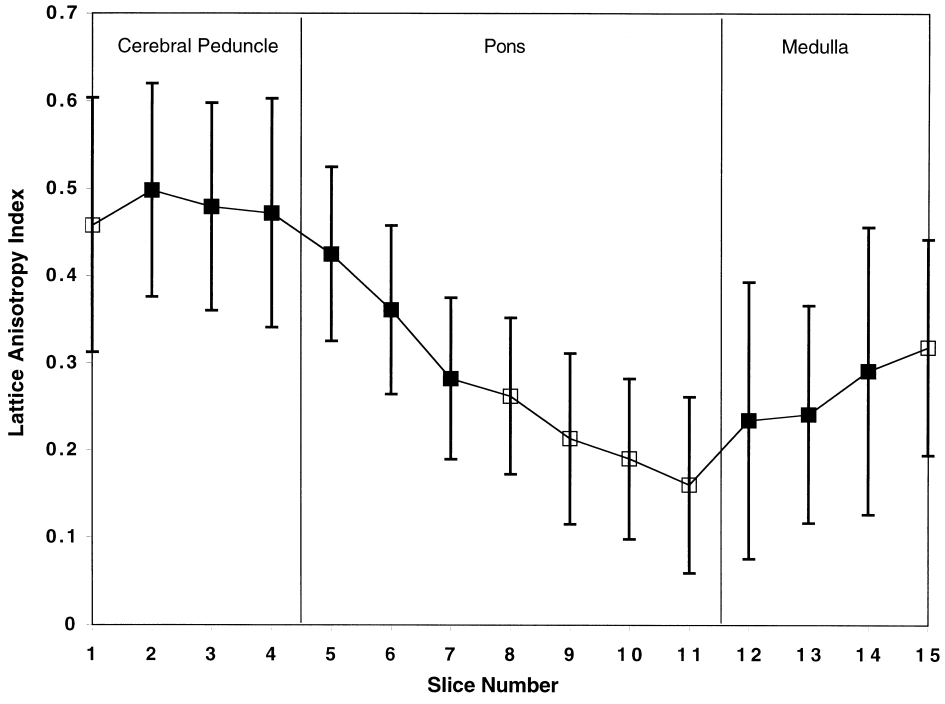

Fig. 2. Representative values of lattice anisotropy index in the pyramidal tract for all brainstem slices imaged in this study. Mean values ± standard deviations from a 71-year-old male subject are shown. The 3.5-mm thick contiguous slices begin at the level of the cerebral peduncle right above the red nucleus (slice number 1) and end in the medulla right above the pyramidal decussation (slice number 15). For each anatomic area, the three slices included in the statistical analysis are indicated by filled squares.

RESULTS

Diffusion anisotropy in the pyramidal tract varied widely at different anatomic levels of the brainstem. In all subjects, regardless of age and gender, anisotropy was clearly higher in the cerebral peduncle than in the pons and medulla (Fig. 2 and Table 1). In each subject, anisotropy had similar average values in all slices at the level of the cerebral peduncle, whereas it varied markedly between consecutive slices in the pons and medulla (Fig. 2). Even in the cerebral peduncle, however, there was a broad distribution of values within the ROI with the lattice anisotropy index ranging between 0.2 and 0.9 (Fig. 3). Lower values were generally found in voxels situated at the periphery of the ROI. Additionally, subjects of the same age and gender sometimes presented markedly different distribution of values in the same anatomic ROI (Fig. 3).

Mean anisotropy values and standard deviations (SDs) for each age, gender, and laterality group in each anatomic area are shown in Table 1. We report the results of the statistical analysis performed using the lattice anisotropy index, however, by using the relative anisotropy index data we found results similar to those obtained with the lattice index. In the following text the first of the two p values reported corresponds to the "individual voxel" analysis, and the second to the "mean value" analysis described in the Materials and Methods. In the cerebral peduncle, anisotropy was slightly but significantly higher in the young than in the elderly (Fig. 4) ($p < 0.0001$, $p = 0.039$), while there were no significant differences between male and female, and left and right side. In the pons, neither age, gender, nor side showed significant effects. In the medulla, anisotropy was slightly higher in the elderly compared to the young ($p = 0.045$, 0.58), and in the male compared to the female ($p = 0.0055$, 0.13). However, these differences were statistically significant only in the "individual voxel" analysis, but not in the "mean value" analysis. Trace (**D**) was higher in the young than in the elderly in the cerebral peduncle ($p < 0.0001$, $p < 0.0001$), pons ($p < 0.0001$, $p < 0.0001$), and medulla ($p < 0.0001$, $p = 0.29$), while there were no differences between left and right and male and female.

We also analyzed the three principal diffusivities (eigenvalues of **D**) in order to better understand the origin of the measured differences in anisotropy. The mean values of the sorted principal diffusivities ± SD for each group in each anatomic area are presented in Table 1. In the cerebral peduncle, the largest principal diffusivity, λ_1, was about 10% higher in the young than in the elderly

Table 1. Values of diffusion tensor-derived quantities in different groups of subjects

	Lattice anisotropy index	Relative anisotropy	Trace (**D**)	λ1	λ2	λ3
Cerebral peduncle						
Young	0.53 ± 0.13	0.53 ± 0.13	2351 ± 110	1595 ± 111	484 ± 59	273 ± 48
Elderly	0.51 ± 0.13	0.50 ± 0.13	2234 ± 169	1460 ± 120	491 ± 71	283 ± 55
Female	0.52 ± 0.13	0.52 ± 0.13	2290 ± 156	1536 ± 142	478 ± 62	277 ± 52
Male	0.52 ± 0.12	0.51 ± 0.13	2294 ± 153	1519 ± 125	497 ± 67	279 ± 51
Right	0.52 ± 0.13	0.52 ± 0.13	2296 ± 161	1537 ± 135	477 ± 56	282 ± 53
Left	0.52 ± 0.13	0.51 ± 0.13	2288 ± 148	1517 ± 132	497 ± 72	274 ± 50
Pons						
Young	0.35 ± 0.12	0.36 ± 0.11	2220 ± 149	1206 ± 102	690 ± 68	324 ± 60
Elderly	0.35 ± 0.12	0.36 ± 0.11	2072 ± 118	1129 ± 95	628 ± 60	316 ± 57
Female	0.35 ± 0.12	0.36 ± 0.11	2146 ± 143	1172 ± 101	657 ± 62	318 ± 55
Male	0.35 ± 0.12	0.36 ± 0.11	2146 ± 164	1164 ± 111	661 ± 79	322 ± 62
Right	0.35 ± 0.12	0.36 ± 0.11	2145 ± 159	1166 ± 105	663 ± 80	317 ± 62
Left	0.34 ± 0.12	0.36 ± 0.11	2148 ± 149	1170 ± 107	655 ± 62	323 ± 55
Medulla						
Young	0.31 ± 0.10	0.35 ± 0.11	3348 ± 563	1499 ± 117	715 ± 68	484 ± 47
Elderly	0.32 ± 0.12	0.36 ± 0.14	3213 ± 385	1473 ± 109	678 ± 81	477 ± 59
Female	0.30 ± 0.10	0.35 ± 0.13	3233 ± 542	1483 ± 126	709 ± 72	489 ± 51
Male	0.33 ± 0.12	0.36 ± 0.13	3328 ± 420	1490 ± 100	684 ± 80	472 ± 54

($p < 0.0001$, $p < 0.0001$), the smallest principal diffusivity, λ_3, was slightly lower ($p = 0.03$, $p = 0.28$), while there was no difference in λ_2, the intermediate diffusivity. In the medulla, λ_2 was slightly higher in the young compared to the elderly ($p = 0.01$, $p = 0.06$), and in the female compared to the male ($p = 0.04$, $p = 0.19$), whereas there were no difference in λ_1 and λ_3. Again, these differences in the medulla reached statistical significance only in the "individual voxel" analysis, but not in the "mean value" analysis.

Anisotropy showed a negative correlation with SNR (slope $= -8.8 \times 10^{-4}$, $r^2 = 0.12$, $p = 0.0066$), and a positive correlation with the motion artifact index MA (slope $= 0.012$, $r^2 = 0.11$, $p = 0.0096$) (Fig. 5). There was no difference in SNR or MA between young and elderly subjects. SNR was significantly lower ($p = 0.0003$), and MA was significantly higher ($p = 0.032$) in the male than in the female group.

DISCUSSION

Diffusion tensor MRI provides parameters that reflect intrinsic diffusivity properties of the tissue and are independent of the subject' s orientation in the magnet.[1] Clinically, this should facilitate quantitative comparison of data acquired in different subjects as well as of data acquired in the same subject at different time points. However, methodological aspects of data acquisition and analysis can critically affect the results of a group analysis of diffusion tensor data in general, and diffusion

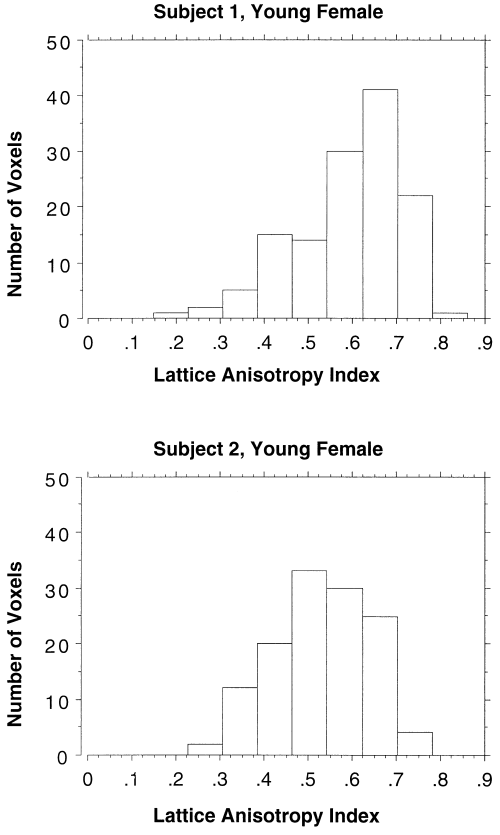

Fig. 3. Histogram of lattice anisotropy index values at the level of the cerebral peduncle in two young female subjects. Distribution of the lattice anisotropy index values varied markedly among subjects in the same age and gender group.

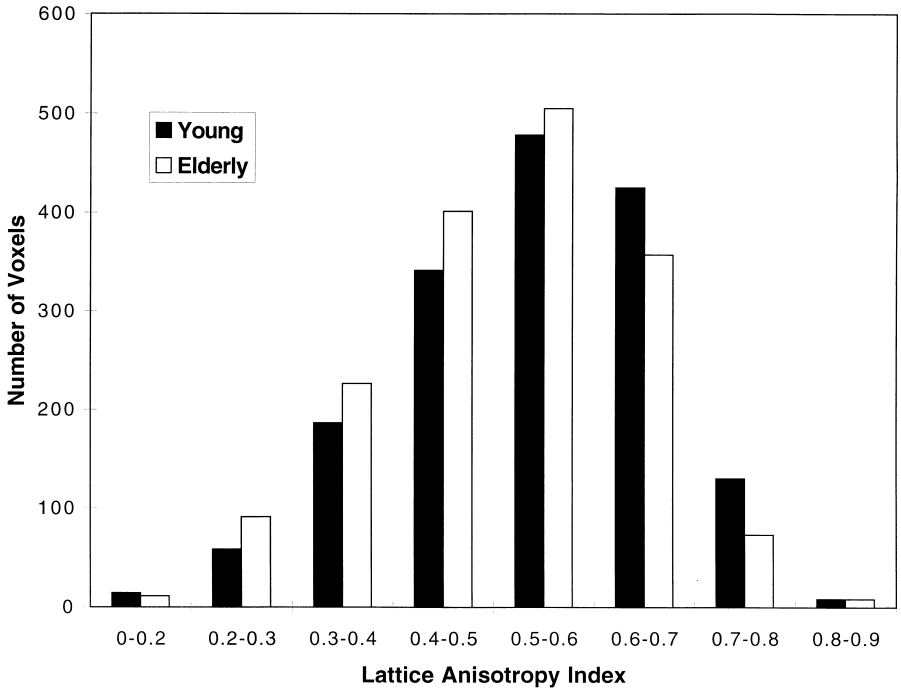

Fig. 4. Histogram of all lattice anisotropy index values measured in the young and elderly volunteers at the level of the cerebral peduncle. While the total number of anisotropic voxels is not markedly different between the two populations, the distribution is shifted toward lower anisotropy values in the elderly.

anisotropy data in particular. Before discussing the biologic findings of our study we will address some of these methodological aspects such as the criteria chosen to define the anatomic region of interest and the approach used for statistical analysis. We will also discuss some general issues related to the biologic interpretation of diffusion anisotropy data.

Definition of the Anatomic ROI

Determining the boundaries of the structure of interest, and avoiding partial volume contamination from neighboring structures are common problems in quantitative image analysis. Although the pyramidal tract in the brainstem is generally well identified on anisotropy maps (see Fig. 1), precisely defining its boundaries with adjacent structures is difficult. Partial volume contamination can originate from surrounding isotropic tissue such as CSF and gray matter, and, in regions such as the pons, from other neighboring white matter structures. We used objective criteria (see Materials and Methods section) to define the boundaries of our structure of interest, such as Trace(**D**) to exclude CSF, and the directional information contained in the eigenvectors of **D** to exclude voxels containing anisotropic fibers not belonging to the pyramidal tract. We chose this approach rather than relying entirely on visual inspection to reduce the possibility that eventual differences between groups could originate from operator-induced bias in defining the ROI. Since diffusion anisotropy in the brain varies widely among different structures, its measurement depends critically on the approach chosen to define the ROI. For example, Pierpaoli et al.[8] measured the anisotropy in the pyramidal tract of normal young subjects using a similar diffusion tensor protocol but including in the analysis only voxels in the center of the structure being investigated. This previous study reported a lattice anisotropy index value of 0.73 ± 0.06 at the level of the cerebral peduncle, which is almost 40% higher than our measurement of 0.53 ± 0.13. This discrepancy is essentially explained by differences in the approach used to determine the ROI. In fact, voxels with the highest anisotropy values are typically located in the center of the fiber structure, while low values are observed in the periphery. Voxels with low anisotropy suffer from partial volume contamination from the surrounding isotropic tissue, whereas voxels with high anisotropy (0.6 to 0.9) most likely include only white matter fibers.

We underscore that in using diffusion anisotropy information clinically, it is essential to agree upon uniform standards for image analysis. In the absence of uniform criteria it will be difficult to carry out multicenter studies of diffusion anisotropy or even compare literature data

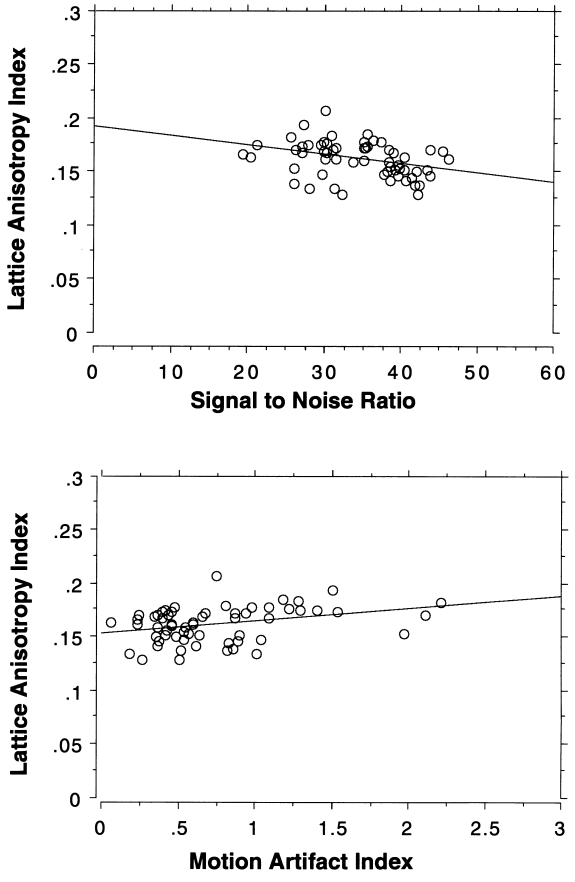

Fig. 5. Linear regression plots of lattice anisotropy index vs. signal to noise ratio (SNR) (upper panel), and lattice anisotropy index vs. motion artifact index (MA) (lower panel) for all subjects included in the study. The circles represent the average values of anisotropy, SNR, and MA in the three contiguous slices where the cerebral peduncle ROIs were defined. Anisotropy values were significantly correlated with both SNR and MA.

obtained in different centers. Moreover, since it is very often impossible to achieve a "blind" analysis of imaging data, investigators should be concerned with the risk of operator-induced bias in intergroup analyses.

Statistical Analysis of Anisotropy Data

The main problem with statistical analysis of diffusion anisotropy data are that noise in the diffusion-weighted images not only increases the variance of the measured anisotropy, but also biases its mean value.[10] Specifically, the same structure imaged with low SNR diffusion-weighted images will appear more anisotropic than if imaged with high SNR. Bias also could arise from motion artifacts, although we are unaware of any systematic study that addresses this issue. Our finding of a positive correlation between diffusion anisotropy values and the motion artifact index provides evidence for this proposition.

The most troubling consequence of this noise- and motion-induced bias is that conventional statistical tests cannot be used reliably to assess differences in anisotropy between datasets acquired with different SNR and amounts of ghosting. Since there are no established statistical methods for accounting for these effects, one may use standard statistical tests, such as ANOVA, only to screen for possible intergroup differences. We should never assume, however, that "statistically significant" differences in such tests reflect a true biologic difference without further investigating the possible effects of noise and motion.

To assess intergroup differences, we used two approaches: we performed ANOVA using both the values of all individual voxels within the ROI, and using only the mean value of all voxels within the ROI. These two methods of analysis represent two extremes: the first treats each voxel as an independent observation, while the second treats the entire ROI as a single independent observation. The individual voxel analysis almost certainly overstates the significance of the results, because it assumes that there is no correlation between anisotropy values in different voxels, while actually voxels are spatially correlated. On the other hand, the mean value analysis probably understates the significance because it discards all information about variance of the anisotropy values within the ROI and pools all voxels into one observation.

We decided to analyze our data using these two approaches because both of them have been used to assess intergroup anisotropy differences in previous studies. Voxel by voxel analysis, in particular, appears to be the approach of choice in studies where anisotropy maps from different subjects are warped to a common template.[23] We wanted to test whether in our study these two approaches would lead to similar results. In general, however, we found that the individual voxel analysis was more likely to reveal significant differences than the mean value analysis. We can not exclude that differences significant only in the individual voxel analysis may have a real biologic origin, and that the mean voxel analysis is simply not sensitive enough to detect them. At the same time, we must acknowledge that significant differences found using the mean value analysis should be regarded as more reliable. Further studies are needed to find an optimal approach for statistical analysis of diffusion anisotropy data. It would be desirable to use all the voxels in the ROI, while taking into account the spatial correlation of neighboring voxels.[24]

Biologic Interpretation of Anisotropy Measurements

The biologic determinants of diffusion anisotropy in the white matter are not completely understood, although it appears that both "structural" and "architectural" features of the tissue play a role. Fiber integrity is an important structural feature that one can investigate using diffusion anisotropy.[9] Other microstructural features include degree of tissue hydration, fiber and neuroglial cells packing density, degree of myelination, and fiber diameter. However, it is difficult to assess the extent of the individual contribution of these factors to the measured diffusion anisotropy experimentally. The main architectural feature affecting diffusion anisotropy is the degree of local orientational coherence of the fibers.[8] Regions such as the corpus callosum, internal capsule, and cerebral peduncle, where fibers are coherently oriented within the voxel, have higher anisotropy than regions such as the centrum semiovale and other subcortical areas where there is less coherence in the intravoxel orientation of fibers.[8]

In this work, anisotropy of the pyramidal tract varied markedly between the cerebral peduncle, pons, and medulla (Fig. 2). We believe that this heterogeneity in anisotropy originates from the remarkably heterogeneous architectural features of the pyramidal tract at different anatomic levels of the brainstem. In the cerebral peduncle, anisotropy is high because the fibers are oriented parallel to each other, and there are no other pathways crossing or branching of collaterals. By contrast, in the pons and medulla, anisotropy is relatively low because in the pons, the pyramidal tract splits into multiple bundles interdigitating with the transverse pontine fibers and, in the medulla, fibers are interspersed with various nuclei and roots of cranial nerves. It is also interesting to note that anisotropy was relatively constant at different levels of the cerebral peduncle while in the pons and medulla there were significant differences in anisotropy even between contiguous slices (Fig. 2), reflecting the higher histologic heterogeneity of the pons and medulla compared with the cerebral peduncle.

The high orientational coherence of the fibers at the level of the cerebral peduncle ensures that differences in anisotropy can be attributed to tissue structure rather than architecture. We found a large distribution of anisotropy values within the cross-sectional area of the cerebral peduncle (anisotropy varied from 0.2 to 0.9) (Fig. 3), with the highest values being located in the center of the structure. Histopathological degeneration studies show the presence of "functional" lamination in the cerebral peduncle (i.e., fibers directed to the face and upper limbs are located medially to the fibers directed to the lower limbs.) (See[25] for a review.) However, the anatomic literature does not suggest that "structural" differences accompany this functional arrangement of fibers. Accordingly, the topographic distribution of the anisotropy values found in this study does not show differences in the medial-lateral direction. Instead, the cross-sectional distribution of anisotropy values appears to reflect partial volume contamination from adjacent isotropic structures, as discussed above. Interestingly, however, the number of voxels showing high anisotropy values, which are less likely to be affected by partial volume contamination, varied markedly between different subjects (Fig. 3). This high intersubject variability probably originates from interindividual differences in the number, size, and myelination of the pyramidal tract fibers. These intersubject differences are reported in the anatomic literature.[12]

Intergroup Comparisons in the Cerebral Peduncle

We found that the elderly had lower anisotropy than the young in the cerebral peduncle. Specifically the number of the very high anisotropy voxels (anisotropy range 0.6–0.8) was reduced in the elderly (Fig. 4), indicating that our finding cannot be explained by partial volume contamination. Errors due to subtle anatomic mismatching are negligible because anisotropy was relatively constant in the consecutive slices in the cerebral peduncle. Neither noise nor motion appears to play a role in this finding because there were no differences in the SNR and MA between young and elderly subjects. Moreover, the differences were statistically significant using both the individual voxel and the mean value analysis. Finally, histopathological studies suggest changes in aging white matter that are consistent with diffusion changes found in this study. The eigenvalues of **D** show that, in the elderly, anisotropy is reduced mostly because water diffusivity parallel to the fibers (λ_1) is decreased. This type of change in the displacement profile of the water molecules could arise from a relative decrease of the volume fraction of the anisotropic tissue (i.e., axons) in the voxel. Histopathological studies have shown diffuse myelin pallor,[13] and loss of small myelinated fibers[26,27] in the aged white matter. Similarly, a recent autopsy study of the corticospinal tract in the spinal cord reported that the density of the small myelinated fibers decreased due to aging.[28] According to Meier-Ruge et al.,[27] part of the volume loss caused by the loss of fibers was compensated by an increased volume of extracellular matrix whereas other studies have found subtle reactive gliosis.[29,30] Decreased number of small myelinated fibers accompanied by reactive gliosis or increased extracellular matrix could explain the decreased anisotropy in the elderly. However, age-related changes in the water content could also contribute to the measured decreased diffusivity parallel to the fibers. Reduced overall concentration of tissue water mainly affects the relatively mobile "free" water pool rather than the more hindered "bound" water associated with macromolecules. The re-

duced concentration of "free" water, in turn, will result in decreased measured diffusivity, more remarkable in the direction parallel to the fibers because of the absence of membranes or other barriers. A recent in vivo spectroscopy study has indeed shown that the brain tissue water content is decreased in the elderly compared to the young.[31] In addition, our study demonstrates that the elderly had lower Trace(**D**) than the young, a finding consistent with decreased concentration of tissue water in the elderly.

Intergroup Comparisons in the Pons and Medulla

In the pons we found no differences between groups. In the medulla we found statistically higher anisotropy in the elderly compared to young subjects, and in males compared to females using the "individual voxel analysis," and no differences between groups using the "mean value" analysis. Taken at face value and interpreted uncritically, these results contradict our findings in the cerebral peduncle. If we assume that reduced anisotropy in the cerebral peduncle indicates fiber degeneration, it is difficult to understand why in elderly subjects, pyramidal tract fibers which are partially degenerated at the level of the cerebral peduncle (decreased anisotropy), appear to regenerate at the level of the medulla oblongata (unchanged or increased anisotropy). One might even suggests that since at the level of the cerebral peduncle the pyramidal tract contains both corticopontine and corticospinal fibers, while in the medulla it contains only corticospinal fibers, aging is associated with selectively reduced corticopontine connectivity compensated by preserved or even increased corticospinal connectivity! Imaginative inferences like these can arise from an uncritical interpretation of "statistically significant" intergroup differences in anisotropy.

When interpreting the results in both the pons and medulla, one must remember that in these two regions, pyramidal tract fibers are interspersed with other fibers which have different orientation. The presence of different fibers with different orientation within a voxel complicates data interpretation because both "microstructural" and "architectural" changes may contribute to the observed anisotropy change. For example, it was recently reported that Wallerian degeneration of pyramidal tract fibers in chronic stroke patients consistently results in decreased anisotropy in the cerebral peduncle, while it may result in slightly reduced, normal, or even increased anisotropy in the pons.[9]

Moreover, there are several other factors that make the anisotropy findings in the medulla less reliable than those in the cerebral peduncle. First, in the medulla the cross-sectional area of the pyramidal tract is very small, and the level of partial volume contamination from the surrounding CSF is high. Second, since in the medulla anisotropy varied markedly between contiguous slices, even a subtle anatomic mismatching of the selected ROI in different patients might have critically affected the analysis. Third, the medulla is situated close to structures such as the cerebellar tonsils, which have a very high degree of motion as result of cardiac pulsation,[32] which in turn could induce motion artifacts in the measurements performed in the medulla. Fourth, the apparently higher anisotropy found in the male subjects as compared to female subjects, could be related to the fact the DWIs acquired in male subjects had a lower SNR and a higher degree of motion artifacts than those acquired in female subjects. Finally, the analysis of the eigenvalues of **D** shows somewhat puzzling changes due to age and gender in the medulla. The diffusivity was higher in one of the two axes perpendicular to the pyramidal tract (λ_2) in the young compared to the elderly and in the female compared to the male, while the diffusivity parallel to the pyramidal tract (λ_1) showed no intergroup difference. These changes are difficult to explain biologically in light of previous histopathological studies on aging white matter.

CONCLUSIONS

Diffusion tensor MRI[1] allows the quantitative assessment of the intrinsic diffusion properties of tissues, independent of the orientation of the subject in the magnet. Theoretically, this should facilitate the clinical use of diffusion imaging by enabling the creation of normative databases and the comparison between results obtained in different studies.

Our study, however, shows that methodological factors, which could be mistakenly regarded as experimental details, critically affect the results and therefore the conclusions of a diffusion tensor study. Since noise in the diffusion weighted images and subject's motion introduce bias in diffusion anisotropy measurements, the finding of "statistically significant" differences in diffusion anisotropy is *per se* meaningless if the effect of these confounding factors cannot be ruled out. Moreover, some aspects of the statistical analysis of diffusion anisotropy measures, such as the effects of the spatial correlation between voxels, require further characterization. We have also shown that the regional variability in diffusion anisotropy, even for a relatively well-defined pathway such as the pyramidal tract, is very large. Therefore, possible anatomic mismatch should be considered in intersubject or intergroup comparisons. Additionally, results are profoundly affected by the criteria chosen to define the ROI. Finally, our study underscores the difficulty of interpreting diffusion anisotropy changes in regions where the intravoxel orientation of anisotropic fibers is not coherent. In addition to the possible influ-

ence of experimental artifacts described above, one should always consider the underlying "architecture" of the tissue under investigation when interpreting diffusion anisotropy results. In our study, only the cerebral peduncle is an ideal region to investigate potential "structural" changes of the pyramidal tract because the fibers are coherently oriented. Since at the level of the cerebral peduncle we have reasonably excluded an artifactual origin of our findings, we believe that the differences in anisotropy between young and elderly subjects truly reflect subtle microstructural changes of the aging white matter.

Recent reports in the literature describe the clinical application of diffusion tensor techniques to investigate very challenging questions about brain connectivity.[23] While it is likely that even subtle structural and architectural changes in the brain could be reflected by an abnormal diffusion behavior of tissue water, we suggest caution in assuming that small differences in diffusion anisotropy have biologic significance if the above experimental and methodological aspects have not received adequate consideration in the study design and data analysis.

Acknowledgments—The authors thank Jeanette Black and Renee' Hill for their assistance in scanning the volunteers, and Andrew E. Schulman, Ph.D., for fruitful discussions on possible approaches for the statistical analysis of the data. The skillful editing of Devera G. Schoenberg, M.S., is also appreciated.

REFERENCES

1. Basser, P.J.; Mattiello, J.; LeBihan, D. MR diffusion tensor spectroscopy and imaging. Biophys. J. 66:259–267; 1994.
2. Basser, P.J. Inferring microstructural features and the physiological state of tissues from diffusion-weighted images. NMR Biomed. 8:333–344; 1995.
3. van Gelderen, P.; de Vleeschouwer, M.H.; DesPres, D.; Pekar, J.; van Zijl, P.C.; Moonen, C.T. Water diffusion and acute stroke. Magn. Reson. Med. 31:154–163; 1994.
4. Ulug, A.M.; Beauchamp, N., Jr.; Bryan, R.N.; van Zijl, P.C. Absolute quantitation of diffusion constants in human stroke. Stroke 28:483–490; 1997.
5. Neil, J.J.; Shiran, S.I.; McKinstry, R.C.; et al. Normal brain in human newborns: Apparent diffusion coefficient and diffusion anisotropy measured by using diffusion tensor MR imaging. Radiology 209:57–66; 1998.
6. Huppi, P.S.; Maier, S.E.; Peled, S.; et al. Microstructural development of human newborn cerebral white matter assessed in vivo by diffusion tensor magnetic resonance imaging. Pediatr. Res. 44:584–590; 1998.
7. Baratti, C.; Barnett, A.; Pierpaoli, C. Comparative MRI study of brain maturation in kittens using T_1, T_2, and the trace of the diffusion tensor. Radiology 210:133–142; 1999.
8. Pierpaoli, C.; Jezzard, P.; Basser, P.J.; Barnett, A.; Di Chiro, G. Diffusion tensor MR imaging of the human brain. Radiology 201:637–648; 1996.
9. Pierpaoli, C.; Barnett, A.; Virta, A.; Penix, L.; Chen, R. Diffusion MRI of Wallerian degeneration. A new tool to investigate neural connectivity *in vivo*? ISMRM Proceedings, Sydney; 1998: 1247.
10. Pierpaoli, C.; Basser, P.J. Toward a quantitative assessment of diffusion anisotropy [published erratum appears in Magn. Reson. Med. 1997 Jun;37(6):972]. Magn. Reson. Med. 36:893–906; 1996.
11. Lassek, A.R., Rasmussen, G.L. The human pyramidal tract. A fiber and numerical analysis. Arch. Neurol. Psychiatry 42:872–876; 1939.
12. Nyberg-Hansen, R.; Rinvik, E. Some comments on the pyramidal tract, with special reference to its individual variations in man. Acta. Neurol. Scand. 39:1–30; 1963.
13. Kemper, T. Neuroanatomical and neuropathological changes during aging and dementia. In: M. L. Albert, J. E. Knoefel, (Eds). Clinical Neurology of Aging. New York: Oxford University Press, 1994: pp. 3–67.
14. Wahlund, L.O.; Almkvist, O.; Basun, H.; Julin, P. MRI in successful aging, a 5-year follow-up study from the eighth to ninth decade of life. Magn. Reson. Imaging 14:601–608; 1996.
15. Salonen, O.; Autti, T.; Raininko, R.; Ylikoski, A.; Erkinjuntti, T. MRI of the brain in neurologically healthy middle-aged and elderly individuals. Neuroradiology 39:537–545; 1997.
16. Anderson, A.W.; Gore, J.C. Analysis and correction of motion artifacts in diffusion weighted imaging. Magn. Reson. Med. 32:379–387; 1994.
17. Ordidge, R.J.; Helpern, J.A.; Qing, Z.X.; Knight, R.A.; Nagesh, V. Correction of motional artifacts in diffusion-weighted MR images using navigator echoes. Magn. Reson. Imaging 12:455–460; 1994.
18. Barnett, A. Improved recontruction algorithm for navigator corrected diffusion weighted interleaved echo-planar images. ISMRM Proceedings, Vancouver; 1997: 1727.
19. Jezzard, P.; Barnett, A.S.; Pierpaoli, C. Characterization of and correction for eddy current artifacts in echo planar diffusion imaging. Magn. Reson. Med. 39:801–812; 1998.
20. Mattiello, J.; Basser, P.J.; Le Bihan, D. The b matrix in diffusion tensor echo-planar imaging. Magn. Reson. Med. 37:292–300; 1997.
21. Basser, P.J.; Pierpaoli, C. Microstructural and physiological features of tissues elucidated by quantitative-diffusion-tensor MRI. J. Magn. Reson. B:209–219; 1996.
22. Pierpaoli, C. Oh no! One more method for molor mapping of fiber tract direction using diffusion MR imaging data. ISMRM Proceedings, Vancouver; 1997: 1741.
23. Buchsbaum, M.S.; Tang, C.Y.; Peled, S.; et al. MRI white matter diffusion anisotropy and PET metabolic rate in schizophrenia. Neuroreport 425–430; 1998.
24. Cressie, N. Statistics for Spatial Data. New York. Wiley, 1993.
25. Nathan, P.W.; Smith, M. Long descending tracts in man. Review of present knowledge. Brain 78:248–303; 1955.
26. Tang, Y.; Nyengaard, J.R.; Pakkenberg, B.; Gundersen, H.J. Age-induced white matter changes in the human brain:

A stereological investigation. Neurobiol. Aging 18:609–615; 1997.
27. Meier-Ruge, W.; Ulrich, J.; Bruhlmann, M.; Meier, E. Age-related white matter atrophy in the human brain. Ann. NY Acad. Sci. 673:260–269; 1992.
28. Terao, S.; Sobue, G.; Hashizume, Y.; Shimada, N.; Mitsuma, T. Age-related changes of the myelinated fibers in the human corticospinal tract: A quantitative analysis. Acta Neuropathol (Berl) 88:137–142; 1994.
29. Beach, T.G.; Walker, R.; McGeer, E.G. Patterns of gliosis in Alzheimer's disease and aging cerebrum. Glia 2:420–436; 1989.
30. Grafton, S.T.; Sumi, S.M.; Stimac, G.K.; Alvord, E.C., Jr.; Shaw, C.M.; Nochlin, D. Comparison of postmortem magnetic resonance imaging and neuropathologic findings in the cerebral white matter. Arch. Neurol. 48:293–298; 1991.
31. Chang, L.; Ernst, T.; Poland, R.E.; Jenden, D.J. In vivo proton magnetic resonance spectroscopy of the normal aging human brain. Life Sci. 58:2049–2056; 1996.
32. Enzmann, D.R.; Pelc, N.J. Brain motion: Measurement with phase-contrast MR imaging. Radiology 185:653–660; 1992.